

UCLA

UCLA Previously Published Works

Title

Ogg1-Dependent DNA Repair Regulates NLRP3 Inflammasome and Prevents Atherosclerosis

Permalink

<https://escholarship.org/uc/item/8cf5k240>

Journal

Circulation Research, 119(6)

ISSN

0009-7330

Authors

Tumurkhuu, Gantsetseg
Shimada, Kenichi
Dagvadorj, Jargalsaikhan
[et al.](#)

Publication Date

2016-09-02

DOI

10.1161/circresaha.116.308362

Peer reviewed



Published in final edited form as:

Circ Res. 2016 September 2; 119(6): e76–e90. doi:10.1161/CIRCRESAHA.116.308362.

Ogg1-Dependent DNA Repair Regulates NLRP3 Inflammasome and Prevents Atherosclerosis

Gantsetseg Tumurkhuu¹, Kenichi Shimada¹, Jargalsaikhan Dagvadorj¹, Timothy R. Crother¹, Wenxuan Zhang¹, Daniel Luthringer², Roberta A. Gottlieb³, Shuang Chen^{1,3}, and Moshe Arditi^{1,4}

¹Departments of Pediatrics, Biomedical Sciences, and Infectious and Immunologic Diseases Research Center (IIDRC), Cedars-Sinai Medical Center, Los Angeles, CA 90048

²Department of Pathology, Cedars-Sinai Medical Center, Los Angeles, CA 90048

³Department of Medicine, Barbra Streisand Women's Heart Center, Heart Institute of Cedars-Sinai, Cedars-Sinai Medical Center, Los Angeles, CA 90048

⁴David Geffen School of Medicine, UCLA, Los Angeles, CA 90048, USA

Abstract

Rationale—Activation of NLRP3 inflammasome mediating IL-1 β secretion has emerged as an important component of inflammatory processes in atherosclerosis. Mitochondrial DNA (mtDNA) damage is detrimental in atherosclerosis and mitochondria are central regulators of the NLRP3 inflammasome. Human atherosclerotic plaques express increased mtDNA damage. The major DNA glycosylase OGG1, is responsible for removing the most abundant form of oxidative DNA damage.

Objective—To test the role of OGG1 in development of atherosclerosis in mouse.

Methods and Results—We observed that Ogg1 expression decreases over time in atherosclerotic lesion macrophages of Ldlr KO mice fed a western diet. Ogg1^{-/-}Ldlr^{-/-} mice fed a western diet resulted in an increase in plaque size and lipid content. We found increased oxidized mtDNA, inflammasome activation, and apoptosis in atherosclerotic lesions and also higher serum IL-1 β and IL-18 in Ogg1^{-/-}Ldlr^{-/-} mice compared with Ldlr^{-/-}. Transplantation with Ogg1^{-/-} bone marrow (BM) into Ldlr^{-/-} mice led to larger atherosclerotic lesions and increased IL-1 β production. However, transplantation of Ogg1^{-/-}Nlrp3^{-/-} BM reversed the Ogg1^{-/-} phenotype of increased plaque size. Ogg1^{-/-} macrophages showed increased oxidized mtDNA and had greater amounts of cytosolic mtDNA and cytochrome c, increased apoptosis, and more IL-1 β secretion. Finally, we found that proatherogenic miR-33 can directly inhibit human OGG1 expression and indirectly suppress both mouse and human OGG1 via AMPK.

Address correspondence to: Dr. Moshe Arditi, Cedars-Sinai Medical Center, Department of Biomedical Sciences, Division of Pediatric Infectious Diseases and Immunology, 8700 Beverly Boulevard, Room 4221, Los Angeles, CA 90048, Tel: 310-423-2593, moshe.arditi@cshs.org.

S.C. and M.A. contributed equally to this work.

DISCLOSURES

None.

Conclusions—OGG1 plays a protective role in atherogenesis by preventing excessive inflammasome activation. Our study provides insight into a new target for therapeutic intervention based on a link between oxidative mtDNA damage, OGG1, and atherosclerosis via NLRP3 inflammasome.

Keywords

Ogg1; atherosclerosis; DNA repair; mitochondria; inflammasome; macrophage

Subject Terms

Vascular Disease; Atherosclerosis; Animal Models of Human Disease; Inflammation

INTRODUCTION

Atherosclerosis is a chronic inflammatory disease that arises from an imbalance in lipid metabolism and a maladaptive immune response driven by the accumulation of cholesterol-laden macrophages in the artery wall. Rupture of atheromatous lesions results in thrombotic occlusion of coronary and cerebral vessels, producing the clinical complications of atherosclerosis^{1, 2}. There is a growing understanding that blood monocytes are recruited to the inflamed vascular wall develop into inflammatory macrophages (M1-like phenotype) and foam cells, which contribute to pathogenesis at many stages of this disease and, therefore, represent a target for therapeutic interventions^{3, 4}. In addition to hyperlipidemia and other genetic factors, inflammation is now known as a critical contributor to atherogenesis. The activation of NLRP3 inflammasome mediating IL-1 β secretion has recently emerged as an important component of inflammatory processes underlying atherosclerosis⁵⁻⁷. The NLRP3 inflammasome can be activated by many diverse danger signals and mitochondria (mt) function as the central hub for integrating these various signals^{5, 8, 9}. We recently showed that during apoptosis/pyroptosis, mitochondrial DNA (mtDNA) damaged by oxidative stress activates the NLRP3 inflammasome, releasing active IL-1 β ¹⁰. Mt are a major site of ROS production and mtDNA is a vulnerable target for ROS-mediated oxidative damage due to its close proximity and the lack of protective histones. Human atherosclerotic plaques showed increased mtDNA damage compared with normal vessels and leukocyte mtDNA damage was associated with higher-risk plaques^{11, 12}.

Oxidative damage in DNA is repaired primarily via the enzymes of the base excision repair (BER) pathway. Among these, OGG1, the major DNA glycosylase, is responsible for removal of 7,8-dihydro-8-oxo-2'-deoxyguanosine (8-OH-dG), one of the most frequent endogenous base lesions formed in the DNA of aerobic organisms¹³. OGG1 deficiency leads to elevated levels 8-OH-dG in mtDNA^{14, 15}. In contrast, mitochondrial overexpression of *Ogg1* improves mitochondrial function, cell survival and fewer mtDNA deletions through increased repair of 8-OH-dG under oxidative stress conditions in vitro¹⁶. A recent study reported in an abstract format showed that loss of OGG1 led to increased apoptosis and larger fatty streaks in mice on western diet and overexpression of *Ogg1* reversed this phenotype, suggesting that *Ogg1* may play a protective role in atherosclerosis¹⁷.

MicroRNAs (miRNAs) are critical post-transcriptional regulators of their target genes. miR-33 targets a number of genes involved in regulating cellular cholesterol export and fatty acid oxidation, including *Prkaa1* (protein kinase, AMP-activated, alpha 1 catalytic subunit) whose gene product is commonly referred to as AMPK α 1 (5' AMP-activated protein kinase alpha subunit 1), which is a metabolic master switch and a target of several drugs used for metabolic diseases in patients^{18–20}. Interestingly, AMPK also regulates *Ogg1* expression²¹. Antagonizing miR-33a/b may be an effective strategy for raising plasma HDL levels and protecting against atherosclerosis in mice and non-human primates^{22, 23}.

In this work, we show the atheroprotective role of OGG1 in a western diet-induced model of atherosclerosis using *Ldlr*^{-/-} mice. The loss of OGG1 resulted in increased mtDNA damage, increased NLRP3 inflammasome activation in macrophages, increased IL-1 β production, and more apoptosis in atherosclerotic plaques, which led to accelerated atherogenesis. NLRP3 deficiency counteracted the loss of OGG1, evidenced by smaller atheromatous plaque lesions.

METHODS

Animals and diets

Ogg1^{-/-} mice were kindly provided from Dr. Christi A. Walter (Univ. Texas Health Science Center at San Antonio). *Nlrp3*^{-/-} mice were provided by Dr. K. A. Fitzgerald (University of Massachusetts Medical School, Worcester, MA). We have crossed for at least 8 generations and established *Ogg1*^{-/-}*Ldlr*^{-/-} and *Ogg1*^{-/-}*Nlrp3*^{-/-} DKO mice. Starting at 8 weeks of age, mice were fed a western diet (WD) (TD88137, Harlan Teklad) for 16 weeks. For bone marrow (BM) transplantation, BM from *Ogg1*^{-/-}, WT, and *Ogg1*^{-/-}*Nlrp3*^{-/-} mice was transplanted into irradiated *Ldlr*^{-/-} mice. After recovery (8 wks), chimeric mice were placed on a WD for 12 wks. Whole blood was collected to confirm the efficiency of the BM transplant. All animal experimental procedures were conducted in strict compliance with the policies on animal welfare of the National Institute of Health. The protocol was approved by the Animal Care and Use Committee at Cedars-Sinai Medical Center.

Assessment of atherosclerotic lesions in the aorta and aortic sinus

The aortas were dissected and the adherent (adventitial) fat was gently removed. Whole aortas were opened longitudinally from the aortic arch to the iliac bifurcation, mounted en face, and stained for lipids with Oil Red O. Hearts were embedded in OCT (Tissue-Tek; Sakura, Torrance, CA) and serial 7 μ m-thick cryosections from the aortic sinus were mounted and stained with Oil Red O and hematoxylin. Image analysis was performed by a trained observer blinded to the genotype of the mice. Representative images were obtained and lesion areas were quantified with Image analysis software using a BZ-9000 microscope (Keyence, Itasca, IL). The lesion area in the aorta *en face* preparations was expressed as a percent of the aortic surface area, as previously reported. The lesion area and lipid-stained areas in the aortic sinus were measured²⁴.

Immunofluorescent analysis of cryosections of the aortic sinus

Apoptotic cells in lesions were detected by TUNEL after proteinase K and EDTA treatment, using the In Situ Cell Death Detection Kit (Millipore). Caspase-1 activity was detected by FLICA staining. For Immunohistochemical staining for frozen sections, fixing and antigen blocking was performed using immunoglobulin from the species of the secondary antibodies. Next, the sections were incubated with primary antibodies overnight at 4 °C, followed by incubation with an appropriate secondary antibodies conjugated with fluorescent dyes. For assessment of macrophage co-localization, macrophages were detected using anti-F4/80 antibody (eBioscience), and anti-CD45 (eBioscience); nuclei were counterstained with DAPI. For some analysis anti-8OH-dG (Bioss) was used, along with anti-TOM20 (Santa Cruz, CA). Images were captured using BZ-9000 microscope (Keyence, Itasca, IL) and analyzed by BZ analyzer software.

Laser-capture microdissection (LCM)

Laser-capture microdissection was performed using a LMD instrument (Leica LMD 700, Leica Biosystem) as previously described²⁵. To visualize F4/80⁺ cells, a guide slide was prepared by staining for F4/80 as described above. Cells corresponding to F4/80⁺ area in serial sections were collected, and RNA was extracted using the RNA Isolation Kit (Clontech). cDNA was synthesized and SYBR Green 2xPCR mixture (Clontech) was used in qPCR according to the manufacturer's instructions. *Ogg1* primers: Fw: 5' - tgtgtaccgaggagacgaca-3', Rv: 5' - ctgtgccaggctgacatcta -3'.

Statistics

All data are expressed as means \pm SD. Statistical differences were measured using either an unpaired Student t test or 1-way analysis of variance (ANOVA) when appropriate with Tukeys post-hoc test. In some cases, the area under the curve was determined, followed by one-way ANOVA with Tukeys post-hoc test. A P value of ≤ 0.05 was considered statistically significant. Data analysis was performed using Prism software version 5.0a (GraphPad, San Diego, CA). Asterisks in the figures represent the following: *: P ≤ 0.05 ; **: P ≤ 0.01 ; and ***: P ≤ 0.001 .

See online Supplement for remaining Methods.

RESULTS

OGG1 deficiency promotes apoptotic and inflammatory responses in macrophages

Somatic mtDNA damage has been reported to accumulate with ageing associated coronary atherosclerotic heart disease²⁶. OGG1 removes the most common oxidative DNA lesion, 8-OH-dG, which we have previously linked to NLRP3 inflammasome activation¹⁰. We wanted to determine the effect of OGG1 deficiency on oxidized mtDNA damage in macrophages. *Ogg1*^{-/-} bone marrow derived macrophages (BMDM) treated with menadione, a ROS inducer, had greater amounts of oxidative damage in their mtDNA as measured by 8-OH-dG dot blot analysis compared with WT BMDMs (Figure 1A). Failure to repair oxidative DNA damage in OGG1 deficient mice can lead to further mt dysfunction and apoptosis²⁷. We therefore examined the effect of the cytotoxic oxysterol, 7-ketocholesterol (7-KC), which is

found in oxidized LDL and atherosclerotic lesions, on apoptosis²⁸. 7-KC treatment resulted in more cytochrome *c* (cyt *c*) and mtDNA in the cytosol of OGG1 deficient macrophages compared to WT cells (Figure 1B and C). 7-KC can activate the NLRP3 inflammasome^{29, 30}. To assess whether mtDNA defects could promote an inflammatory phenotype caused by 7-KC, we examined caspase1 activation by fluorochrome-labeled inhibitors of caspases assay (FLICA). 7-KC treatment elicited more caspase-1 activation in *Ogg1*^{-/-} macrophages than WT controls (data not shown). We assessed cell viability by MTT assay after incubating with 7-KC for 24 hours. Exposure to 7-KC resulted in a concentration-dependent increase in cell death that was significantly greater in *Ogg1*^{-/-} cells (Figure 1D). The NLRP3 inflammasome is activated by many diverse danger signals and mt function is the central hub for integrating these signals, resulting in inflammation. We previously showed that oxidized mtDNA binds to and activates the NLRP3 inflammasome¹⁰. Thus, in *Ogg1*^{-/-} BMDM, where there is more oxidized mtDNA damage, there should be greater NLRP3 inflammasome activation. BMDM were pretreated with LPS and then stimulated with various NLRP3 activators such as ATP, 7-KC, and cholesterol crystals. *Ogg1*^{-/-} macrophages secreted significantly more IL-1 β , but not TNF- α , compared with WT cells (Figure 1E). We next investigated whether we could rescue this phenotype by adding mitochondrial specific *Ogg1* back into *Ogg1*^{-/-} BMDM. Retrovirus expressing mtOgg1 introduced into the *Ogg1*^{-/-} BMDMs produced less IL-1 β in response to LPS +ATP stimulation compared with control virus transduced cells (Figure 1F). The efficiency of retroviral infection was checked by eGFP expression under fluorescent microscope (Supplemental Figure IA). Taken together, these results indicate that macrophages deficient in OGG1 exhibit greater mitochondrial dysfunction, increased inflammasome activity, and more apoptosis when exposed to 7-ketocholesterol than WT cells.

The expression of OGG1 diminishes as atherosclerotic lesions progress

mtDNA damage has been correlated with the extent of atherosclerosis and usually precedes atherogenesis³¹. Oxidative damage to mtDNA can be detected by strong immunoreactivity for 8-OH-dG, is found in all cell types of the plaque and correlates with atherosclerosis progression^{32, 33}. However, the expression of *Ogg1* in the lesion during diet-induced atherogenesis is not known. At 8 weeks of age, *Ldlr*^{-/-} mice were fed western diet (WD), blood and tissue were harvested at the indicated time points. As expected, serum total cholesterol and aortic root plaque size increased over time (Figure 2A and B). OGG1 was detected in the lesions by immunofluorescence and was readily visible in the lesion after 4 weeks on WD (Figure 2C and D). However, OGG1 protein decreased as the lesion progressed, with staining in few cells by 16 weeks WD. The reduction in OGG1 staining was also specifically observed in F4/80 positive macrophages (Figure 4C and D). Recent studies have found that some smooth muscle cells (SMCs) may upregulate F4/80 on their surface as they become more macrophage like³⁴. However, in our system, the majority of F4/80 positive cells co-expressed CD45, indicative of their hematopoietic origin (Supplemental Figure IIA). We confirmed our immunofluorescence results using laser-capture microdissection (LCM). F4/80⁺ macrophages were isolated from atherosclerotic plaques of *Ldlr*^{-/-} mice fed WD for 4 and 16 weeks. Total RNA was extracted and mRNA expression analysis performed by RT-PCR. Notably, *Ogg1* mRNA expression levels decreased in lesional macrophages at 16 weeks compared with 4 weeks (Figure 2E). Taken

together, these data suggest that *Ogg1* expression diminishes in the plaque lesions generally, and in macrophages specifically, as the atheroma progresses.

OGG1 deficiency leads to accelerated atherosclerosis

To understand the significance of OGG1 in development and progression of atheromas, we generated *Ogg1*^{-/-}*Ldlr*^{-/-} double knockout (DKO) mice and fed them a WD diet for 16 weeks starting at 8 weeks of age. Representative images of the aortic root lesions are shown in Figure 3A. We found that the atherosclerotic lesion area and its macrophage content in cross-sections of the aortic root were increased significantly in *Ogg1*^{-/-}*Ldlr*^{-/-} mice compared with *Ldlr*^{-/-} controls (Figure 3B and C). The critical features of advanced atheromatous lesions are increases in TUNEL positive apoptotic cells and necrotic area^{35, 36}, and a corresponding decrease in collagen content. OGG1 deficiency resulted in a significant increase in both TUNEL positive cells and necrotic area, as well as a decrease in collagen content in their lesions (Figure 3D–F, Supplemental Figure IIB). *En face* analyses of the aorta showed an increase in the total surface area occupied by lesions in DKO mice compared with controls (Figure 3G and H), suggesting the loss of OGG1 accelerates diet-induced atheroma development in *Ldlr*^{-/-} mice. We did observe a gene dose effect as *Ogg1*^{+/-}*Ldlr*^{-/-} mice displayed an intermediate phenotype. Thus OGG1 deficiency leads to larger more advanced atheromatous lesions on the *Ldlr*^{-/-} background.

OGG1 deficiency leads to increased damaged mtDNA (8-OH-dG) and inflammasome activity in atherosclerotic lesions

Since OGG1 removes 8-OH-dG from DNA, we expected that we would find increased accumulation of 8-OH-dG modifications of DNA in the plaques in our *Ogg1*^{-/-}*Ldlr*^{-/-} mice. Immunofluorescence revealed a ~4-fold greater accumulation of 8-OH-dG in the plaques of DKO mice, compared with controls (Figure 4A and B). Using Tom20 as a mitochondrial marker, colocalization analysis indicated that >80% of the 8-OH-dG staining was mitochondrial, implicating mtDNA as the likely target (Figure 4B, Supplemental Figure IIC). Additionally, F4/80 positive macrophages were observed to have increased 8-OH-dG staining in the lesions as well (Figure 4C).

Since we found an increase in 8-OH-dG in the lesions, and concomitantly an increase in apoptotic cells, we reasoned that we would also find an increase in IL-1 β producing cells as apoptotic signals along with oxidized mtDNA can activate the NLRP3 inflammasome¹⁰. To elucidate the contribution of Nlrp3 inflammasome in the accelerated atherogenesis that we observed in OGG1 deficient *Ldlr*^{-/-} mice (DKO mice), caspase-1 activation was investigated by FLICA in lesions of the aortic roots of both groups of mice. Nearly 2-fold more FLICA-positive F4/80⁺ macrophages were detected in the plaques of DKO mice compared with controls (Figure 4D and E). Taken together, these results indicate that the loss of OGG1 results in advanced plaque formation characterized by increased oxidized DNA damage (8-OH-dG), more apoptotic cells, and more cells with active caspase-1, which can produce IL-1 and IL-18, cytokines that are both strongly pro-atherogenic.

Lipid accumulation and cell death within the lesions contribute to activation of inflammatory cells that release proinflammatory and proatherogenic mediators into the serum^{37, 38}.

Additionally, our data suggests increased inflammasome activity in OGG1 deficient mice. Analysis of key cytokines and chemokines in the plasma revealed significantly higher concentrations of IL-1 β , IL-18, and MCP-1 in DKO mice, whereas the concentrations of IL-12p40, IL-6, and TNF- α were indistinguishable between the two groups (Figure 5). Both IL-1 β and IL-18 are dependent on the inflammasome for their secretion.

A prior study reported that *Ogg1*^{-/-} mice may develop metabolic syndrome³⁹. In order to determine if the differences we observed were due to possible metabolic changes, we tested the mice after 16 weeks of WD for glucose tolerance and insulin resistance and found no difference between the genotypes (Supplemental Figure IIIA). The body weight gains and plasma cholesterol levels (triglycerides and lipoprotein profiles) were also similar (Supplemental Figure IIIB and C). Thus, the accelerated atheroma development in the OGG1-deficient mice in this study cannot be attributed to metabolic changes such as more severe dyslipidemia or altered glucose homeostasis.

NLRP3 significantly contributes to OGG1 deficiency-induced acceleration of atherosclerosis in hematopoietic cells

We hypothesized that OGG1 deficiency and the consequent accumulation of 8-OH-dG in mtDNA would result in more NLRP3 inflammasome activation as a critical driver of the accelerated atherosclerosis that we observed. Therefore, we next investigated whether NLRP3 is required for the acceleration of atherosclerosis in *Ogg1*^{-/-} mice. We generated *Ogg1*^{-/-}*Nlrp3*^{-/-} mice, and then created bone marrow (BM) chimeric mice using BM cells from WT, *Ogg1*^{-/-}, *Ogg1*^{-/-}*Nlrp3*^{-/-} or *Nlrp3*^{-/-} mice into *Ldlr*^{-/-} recipient mice and 8 weeks after BM transplant, placed them on WD for 12 weeks. Mice that received *Ogg1*^{-/-} BM developed significantly larger, more complex lesions in aortic root and abdominal aorta than mice receiving WT BM (Figure 6A–E). In agreement with our hypothesis, OGG1 deficiency-accelerated lesion size was reduced in *Ldlr*^{-/-} mice that received OGG1 and NLRP3 doubly deficient BM cells (Figure 6A–E). Indeed, while the lesion size was significantly reduced in the *Ogg1*^{-/-}*Nlrp3*^{-/-} chimeras compared with *Ogg1*^{-/-} alone, there was no significant difference between *Ogg1*^{-/-}*Nlrp3*^{-/-} and *Nlrp3*^{-/-} highlighting the importance of the NLRP3 pathway in the *Ogg1*^{-/-} mice for atherosclerotic lesion size (Figure 6B, E). Finally, *Nlrp3*^{-/-} chimeras alone did not have significantly smaller lesions than WT mice, although they did trend towards a reduction (Figure 6B,C,E), consistent with a recent study⁵.

Consistent with the role of OGG1 to remove oxidized guanine residues, we noted a greater accumulation of 8-OH-dG in the plaques of *Ogg1*^{-/-} and *Ogg1*^{-/-}*Nlrp3*^{-/-} BM chimeras (Figure 6F). The accumulation of 8-OH-dG was not affected by the presence or absence of NLRP3. We then investigated whether we could detect increased amounts of mature IL-1 β in the lesions. *Ldlr*^{-/-} mice that received *Ogg1*^{-/-} BM cells indeed expressed more mature cleaved IL-1 β as compared with WT BM (Figure 6G). Importantly, atheroma development was substantially reduced in the chimeric mice that received *Ogg1*^{-/-}*Nlrp3*^{-/-} BM despite no difference in glucose tolerance, insulin resistance and lipid metabolism compared with the WT chimeras (Supplemental Figure IIID and E). Collectively, these data suggest that

OGG1 deficiency in hematopoietic cells accelerates plaque progression at least partially through the Nlrp3 inflammasome.

miR-33 downregulates OGG1 in human and mouse cells by different mechanisms, leading to increased 8-OH-dG accumulation and IL-1 β production

OGG1 content in the aortic root diminished significantly as atherosclerosis progressed, suggesting that atherosclerosis inversely affected *Ogg1* expression or stability. Therefore, we examined the role of AMPK, an upstream regulator of *Ogg1*²¹. We confirmed that AMPK activation induced *Ogg1* transcription by treating mouse BMDM cells with AICAR and Metformin, both potent AMPK activators. Indeed, both treatments led to increased *Ogg1* mRNA (Figure 7A). We next assessed whether activated AMPK levels changed during atherogenesis. Consistent with the decreased expression of *Ogg1* during atherogenesis, the amount of phospho- and AMPK in aortic arch lysate of *Ldlr*^{-/-} mice a fed a 16 week-WD was also diminished (Figure 7B). Thus it is likely that the decrease in AMPK leads to reduced *Ogg1* expression during atherosclerosis.

Analysis of the 3' UTR regions of human *OGG1* identified putative binding sites for miR-33 at nucleotides 312–318 and 367–373, but not in mouse *Ogg1* (Supplemental Figure IVA). miR-33 is known to play an important pro-atherogenic role, negatively affecting lipid metabolism and cholesterol export, as well as the master regulatory switch AMPK^{40–42}. We therefore asked if these miR-33 binding sites were functional and regulated OGG1 levels in the cell either directly, or through AMPK. miR-33 mimics as well as their specific inhibitors were transfected into both human and mouse cells to test for their effects on *OGG1* expression. As predicted, densitometric quantification of OGG1 protein amounts normalized by GAPDH amounts showed that the miR-33 mimics were able to inhibit *OGG1* expression in HeLa cells, but not in B6-MCL cells (Figure 7C, Supplemental Figure IVB), suggesting that miR-33a could directly regulate human *OGG1*, but not mouse *Ogg1*. This was especially the case for miR-33-5p, while miR-33-3p was less effective in its inhibition. Inclusion of the mimic inhibitors abrogated the effects of the miR-33 mimics (Figure 7C and D). Next we assessed protein expression by treating the cells with 1 mM AICAR (AMPK activator) for 2h, and observed that this led to increased phosphorylation of AMPK α as well as increased expression of *Ogg1*, but the addition of miR-33-3p and -5p mimics significantly inhibited them in both human and mouse cells (Figure 7C and D). As before, co-transfection of miR-33-3p or -5p specific inhibitors reversed the effect of miR-33-3p and -5p mimics in these cells (Figure 7C and D). To assess the functionality of these sequences, we transfected HEK293 cells with a reporter construct, which expressed a luciferase coding sequence fused to the 3' UTR of *OGG1* (human). Cotransfection of miR-33-3p and -5p mimics markedly suppressed the activity of the *OGG1* 3' UTR luciferase construct, compared with empty vector control (Figure 7E). Next, we examined the effect of miR-33 inhibition on OGG1 activity to repair oxidized DNA damage. HeLa cells were transfected with miR-33-3p and -5p mimic and 48h later, they were treated with 25 μ M of menadione to induce mtROS¹⁶. The level of 8-OH-dG was determined by flow cytometry. We found that menadione treatment led to more 8-OH-dG in miR-33 mimic transfected cells, compared with control cells (Figure 7F). Finally, similar to *Ogg1*^{-/-} macrophages, MCL transfected with miR-33 mimics produced more IL-1 β in response to LPS + ATP stimulation (Figure 7G), but

produced similar amounts of TNF- α . Taken together, these data suggest that miR-33a downregulates *Ogg1* expression through AMPK in both mice and humans, and also directly targets human but not mouse *Ogg1*. Thus reduction in OGG1 by miR-33 leads to increased 8-OH-dG accumulation and greater IL-1 β production.

It was recently reported that miR-33 is upregulated in human atherosclerotic plaques⁴³. As our data showed that OGG1 diminishes over time during atherogenesis in mice, and its expression can be regulated miR-33 and AMPK, we next investigated whether *OGG1* was also reduced in human atherosclerotic plaques. Indeed, in agreement with our mouse data, we found that *OGG1* transcript was indeed reduced in human coronary and carotid plaques compared with normal vessels (Supplemental Figure V).

DISCUSSION

Atherosclerosis is a disease characterized by lipid accumulation in the vessel wall, cell death and chronic inflammation. In our study we found that WD-fed *Ogg1*^{-/-}*Ldlr*^{-/-} mice and *Ogg1*^{-/-} BM chimeric mice developed bigger, more complex lesions with larger necrotic cores. However, this increase was abrogated in *Ogg1*^{-/-}*Nlrp3*^{-/-} BM chimeric mice, suggesting that the mechanism by which *Ogg1* deficiency leads to accelerated atherogenesis is at least in part through the NLRP3 inflammasome. While some human *Ogg1* polymorphisms have been linked with various pathologies such as large artery atherosclerotic stroke in smokers⁴⁴ and SLE severity^{45, 46}, no studies have yet demonstrated its role in atherosclerosis.

Apoptosis in both vascular SMCs and macrophages may promote inflammation and alter plaque composition, although the significance of apoptosis in atherosclerosis depends on the stage of the plaque, localization, and the cell types involved⁴⁷. Previously, *Ogg1* KO mice showed decreased intracellular ATP content⁴⁸ and were more susceptible to apoptosis in response to oxidative stress^{49, 50}. Here, we show that loss of OGG1 in macrophages results in increased mtDNA damage, greater cytochrome *c* release, increased cytosolic mtDNA, and caspase1 activation, leading to increased apoptosis, increased IL-1 β secretion and inflammation. Since intrinsic apoptosis is regulated by mitochondria, mt dysfunction due to mtDNA damage can lead to more cell death^{51, 52}. In the case of atheromas, macrophage apoptosis contributes to necrotic core formation, which can trigger acute thrombotic events^{53, 54}. Apoptotic cells display a variety of recognition signals that lead to their swift removal by professional phagocytes. However, improper removal of these cells can lead to secondary necrosis and subsequent inflammation⁵⁵. As *Ogg1* expression diminishes over time as atherosclerosis progresses, more cell death may occur, resulting in progressively larger necrotic cores.

OGG1 is responsible for repairing 8-OH-dG lesions in DNA, and is particularly important for clearing these lesions from mtDNA. While there is more nuclear DNA in the cell compared with mtDNA, mtDNA is much more susceptible to oxidative damage due to its lack of protective histones and its close proximity to mtROS. Additionally, mitochondria only have base excision repair, of which OGG1 is a member, while the nucleus possesses both base excision repair as well as nucleotide excision repair^{56, 57}. Thus OGG1 deficiency

would likely have a much greater effect on mtDNA than nuclear DNA, with which our data was in agreement. Ogg1 deficiency resulted in a substantial increase in oxidized mtDNA, which resulted in NLRP3 activation, IL-1 β secretion, and accelerated atherosclerosis. Several reports have investigated the causes and pathological consequences of excessive mtROS in atherosclerosis in both humans and mouse models^{36, 58}. It is reported that 8-OH-dG accumulation in mtDNA is increased 20-fold in livers of *Ogg1*^{-/-} mice compared to WT mice⁵⁹. The human Ser326Cys (C8055G) OGG1 polymorphism is associated with decreased repair activity⁶⁰ and is linked to large artery atherosclerotic stroke in smokers⁴⁴; the C1245G polymorphism correlates with increased 8-OH-dG in leukocyte DNA and more severe manifestations of systemic lupus erythematosus (SLE)^{45, 46}. Atherosclerosis is a well-recognized complication of SLE, but underlying mechanisms are complex and remain areas of active investigation. Thus growing evidence supports the potential role of *Ogg1* in modifying atherosclerosis. Oxidation of mtDNA is directly attributed to reactive oxygen species derived from mt respiration, making mitochondria both the source and the target of oxidative stress. Several reports have linked mitochondrial damage to atherosclerosis in both humans and mouse models^{36, 58}. While mtDNA damage might be expected to result in mitochondrial dysfunction including decreased ATP production and increased generation of reactive oxygen species, OGG1-null mice up to the age of 14 months had normal mitochondrial function⁶¹. We suggest that the proatherogenic effect of OGG1 deficiency is more likely to be a consequence of activation of NLRP3 by overabundant 8-OH-dG. Our finding that loss of NLRP3 mitigated the proatherogenic effect of OGG1 deficiency on plaque size supports this notion. The NLRP3 inflammasome is activated by many diverse stimuli making NLRP3 the most versatile and importantly, also the most clinically implicated inflammasome^{62, 63}. Furthermore, IL-1 β is known as a critical component of inflammation that accelerates atherosclerosis⁶⁴⁻⁶⁶, and our data is in agreement with this concept.

It was previously reported that *Ogg1*^{-/-} mice on a WD develop obesity and metabolic syndrome³⁹. However, in our study, the genetic loss of *Ogg1* did not significantly exacerbate metabolic alterations after 16 weeks on WD, compared with *Ldlr*^{-/-} control mice. Importantly, adoptive transfer of *Ogg1*^{-/-} BM cells into irradiated *Ldlr*^{-/-} mice also resulted in increased atherogenesis, increased apoptosis, and increased inflammasome activity, with no changes in metabolic readouts. While our data suggests a strong link between OGG1 and the NLRP3 inflammasome during atherosclerosis, it is also possible that Ogg1 acts through other pathways. Indeed, while lesion size (aortic sinus and aorta *en face*) in *Ogg1*^{-/-} mice seemed to mainly be driven by the NLRP3 pathway, the lipid content of the lesions was increased in *Ogg1*^{-/-} mice, but was not affected by NLRP3 deletion at twelve weeks WD (data not shown) suggesting that OGG1 may affect lipid accumulation in the plaque through a non-NLRP3 inflammasome related pathways. Any new mechanisms by which OGG1 may affect the progress of atherosclerosis that is NLRP3 independent will require further studies.

It is intriguing that another study using an acute injury model, LPS-induced organ failure model, suggested a pro-inflammatory role for OGG1 as *Ogg1*^{-/-} mice had reduced inflammation. The authors, proposed that single strand breaks made by OGG1 in the DNA may serve as a danger signal that induces inflammation in their model of acute inflammation⁶⁷. However, other studies have shown that OGG1 has an anti-inflammatory

effect in different disease models⁶⁸, in agreement with our findings. It could be that the pro- or anti-inflammatory effects of OGG1 are disease dependent with OGG1 being anti-inflammatory in more chronic disorders, such as atherosclerosis, while OGG1 may be pro-inflammatory in certain acute diseases. Further research is required to distinguish between these two possibilities.

The role of miR-33 in atherogenesis has increasingly been recognized^{69–71}. Treatment with miR-33 antagonist oligonucleotide in mouse and nonhuman primates, as well studies in miR-33 KO mice, showed protection against atherosclerosis by increasing reverse cholesterol transport, leading to higher plasma HDL levels⁷². Additionally miR-33α/β was found to be markedly increased in human carotid atherosclerotic plaques compared with normal arteries⁷³. Furthermore, miR-33 controls energy metabolism via repression of key mitochondrial genes to limit ATP production and dampen cholesterol efflux^{74, 75}. Also, miR-33 was shown to skew towards M1 polarization of macrophages, which is proinflammatory and proatherogenic, while antagonism of miR-33 leads to M2 polarization, which is atheroprotective⁷⁵. Mitochondrial activity and macrophage polarization are linked, with miR-33 influencing both processes^{43, 75}. OGG1, which is required for mtDNA repair, may therefore play a regulating role in both these pathways. Finally, miR-33 can also regulate *IIIβ* expression levels in atherosclerotic lesions⁷⁶. However, Goedeke L et al⁷⁷ reported that long-term anti-miR-33 therapy in mice might be associated with side effects such as hypertriglyceridemia and moderate hepatic steatosis, but overall, miR-33 is regarded as a potential therapeutic target for atherosclerosis^{40, 70, 78}. Therefore, it is of great potential interest that in this study we discovered that miR-33 also targets *OGG1* and downregulates its expression directly in human cells, and indirectly in both human and mice.

However, while the complete repertoire of miR-33 target genes is unknown, miR-33 targets a number of metabolic pathways, including AMPKα. The expression of AMPKα is diminished during atherogenesis, which leads to decreased autophagy and paradoxical upregulation of SREBP-1c and SREBP-2, as well as further progression of atherosclerosis^{79, 80}. Restoring AMPKα expression protects from atherogenesis^{81, 82}. Importantly, AMPKα acts upstream of *Ogg1*, thus miR-33 can also act on *Ogg1* indirectly and this pathway is conserved in both humans and mice. Indeed, we also found that *hOGG1* expression was also reduced in human atherosclerotic plaques in diseased arteries compared with normal controls.

Several publications have reported that stress responsive transcription factors, Nrf-2 (nuclear factor erythroid 2 [NF-E2]-related factor 2) and NF-YA (nuclear transcription Y subunit alpha), also regulate *Ogg1* expression^{83, 84}. Coincidentally, they are also regulated by AMPK⁸⁵. Furthermore, NF-Ys function as a heterotrimeric transcriptional complex composed of three subunits, NF-YA, NF-YB, and NF-YC. A recent study showed NF-YC is also a miR-33 target gene as it was markedly increased in mice administered with miR-33 anti-sense oligonucleotide compared to control miRNA-treated mice⁷⁷. Thus it is likely that miR-33 plays an important role *in vivo* controlling *Ogg1* during atherogenesis and further studies are required to understand the complex interaction with miR-33 and *OGG1* during plaque progression.

There is a growing understanding on the key roles of macrophages in the initiation, progression and resolution of atherosclerotic inflammation^{43, 86}. Our study further highlights the importance of macrophages as OGG1 deficiency caused a significant increase in oxidative damage in mtDNA leading to increased caspase 1 activation, most notably in macrophages, leading to greater IL-1 β production and accelerated atherogenesis. Two isoforms of OGG1 protein exist (mitochondrial and nuclear), but the importance of mitochondrial OGG1 in the protection of oxidative stress is clearly demonstrated in this study. Furthermore, mtDNA damage is significantly more abundant and persists longer than nuclear DNA (nDNA) damage following exposure to oxidative stress⁸⁷. Human atheromatous plaques show increased mtDNA damage, particularly associated with higher-risk plaques^{43, 88}. In conclusion, this work provides direct evidence for a causal link between oxidative DNA damage repair enzyme, OGG1, and atherosclerotic plaque development in part via the NLRP3 inflammasome and IL-1 β . Our study reveals a novel therapeutic target to limit oxidative mtDNA damage, which then down-regulates the NLRP3/IL-1 β axis and prevent or treat atherosclerosis.

Supplementary Material

Refer to Web version on PubMed Central for supplementary material.

Acknowledgments

We would like to thank G. Huang and P. Sun for excellent technical assistance.

SOURCES OF FUNDING

This work was supported by the National Institutes of Health Grants AI105845 (to M.A.) and HL111483 (to S.C.).

Nonstandard Abbreviations and Acronyms

| | |
|--------------|---|
| AMPK | AMP-activated protein kinase |
| ATP | Adenosine triphosphate |
| HDL | High-density lipoprotein |
| LDL | Low-density lipoprotein |
| Ldlr | Low density lipoprotein receptor |
| miRNA | microRNA |
| mtDNA | Mitochondrial DNA |
| Nlrp3 | nucleotide binding domain and leucine-rich repeat (NLR) pyrin domain containing 3 |
| Ogg1 | 8-Oxoguanine glycosylase |
| PCR | Polymerase Chain Reaction |
| TG | Triglyceride |

| | |
|----------------|-------------------------------------|
| WD | Western diet |
| 8-OH-dG | 7,8-dihydro-8-oxo-2'-deoxyguanosine |

References

1. Libby P. Inflammation in atherosclerosis. *Nature*. 2002; 420:868–874. [PubMed: 12490960]
2. Moore KJ, Tabas I. Macrophages in the pathogenesis of atherosclerosis. *Cell*. 2011; 145:341–355. [PubMed: 21529710]
3. Moore KJ, Sheedy FJ, Fisher EA. Macrophages in atherosclerosis: A dynamic balance. *Nature reviews Immunology*. 2013; 13:709–721.
4. Woollard KJ, Geissmann F. Monocytes in atherosclerosis: Subsets and functions. *Nat Rev Cardiol*. 2010; 7:77–86. [PubMed: 20065951]
5. Duewell P, Kono H, Rayner KJ, Sirois CM, Vladimer G, Bauernfeind FG, Abela GS, Franchi L, Nunez G, Schnurr M, Espevik T, Lien E, Fitzgerald KA, Rock KL, Moore KJ, Wright SD, Hornung V, Latz E. Nlrp3 inflammasomes are required for atherogenesis and activated by cholesterol crystals. *Nature*. 2010; 464:1357–1361. [PubMed: 20428172]
6. Li X, Zhang Y, Xia M, Gulbins E, Boini KM, Li PL. Activation of nlrp3 inflammasomes enhances macrophage lipid-deposition and migration: Implication of a novel role of inflammasome in atherogenesis. *PLoS one*. 2014; 9:e87552. [PubMed: 24475307]
7. Gage J, Hasu M, Thabet M, Whitman SC. Caspase-1 deficiency decreases atherosclerosis in apolipoprotein e-null mice. *Can J Cardiol*. 2012; 28:222–229. [PubMed: 22265992]
8. Masters SL, Dunne A, Subramanian SL, Hull RL, Tannahill GM, Sharp FA, Becker C, Franchi L, Yoshihara E, Chen Z, Mullooly N, Mielke LA, Harris J, Coll RC, Mills KH, Mok KH, Newsholme P, Nunez G, Yodoi J, Kahn SE, Lavelle EC, O'Neill LA. Activation of the nlrp3 inflammasome by islet amyloid polypeptide provides a mechanism for enhanced il-1beta in type 2 diabetes. *Nature immunology*. 2010; 11:897–904. [PubMed: 20835230]
9. Gurung P, Lukens JR, Kanneganti TD. Mitochondria: Diversity in the regulation of the nlrp3 inflammasome. *Trends in molecular medicine*. 2015; 21:193–201. [PubMed: 25500014]
10. Shimada K, Crother TR, Karlin J, Dagvadorj J, Chiba N, Chen S, Ramanujan VK, Wolf AJ, Vergnes L, Ojcius DM, Rentsendorj A, Vargas M, Guerrero C, Wang Y, Fitzgerald KA, Underhill DM, Town T, Arditi M. Oxidized mitochondrial DNA activates the nlrp3 inflammasome during apoptosis. *Immunity*. 2012; 36:401–414. [PubMed: 22342844]
11. Yu E, Calvert PA, Mercer JR, Harrison J, Baker L, Figg NL, Kumar S, Wang JC, Hurst LA, Obaid DR, Logan A, West NE, Clarke MC, Vidal-Puig A, Murphy MP, Bennett MR. Mitochondrial DNA damage can promote atherosclerosis independently of reactive oxygen species through effects on smooth muscle cells and monocytes and correlates with higher-risk plaques in humans. *Circulation*. 2013; 128:702–712. [PubMed: 23841983]
12. Gray K, Kumar S, Figg N, Harrison J, Baker L, Mercer J, Littlewood T, Bennett M. Effects of DNA damage in smooth muscle cells in atherosclerosis. *Circulation research*. 2015; 116:816–826. [PubMed: 25524056]
13. Dianov G, Bischoff C, Piotrowski J, Bohr VA. Repair pathways for processing of 8-oxoguanine in DNA by mammalian cell extracts. *J Biol Chem*. 1998; 273:33811–33816. [PubMed: 9837971]
14. de Souza-Pinto NC, Eide L, Hogue BA, Thybo T, Stevnsner T, Seeberg E, Klungland A, Bohr VA. Repair of 8-oxodeoxyguanosine lesions in mitochondrial dna depends on the oxoguanine dna glycosylase (ogg1) gene and 8-oxoguanine accumulates in the mitochondrial dna of ogg1-defective mice. *Cancer Res*. 2001; 61:5378–5381. [PubMed: 11454679]
15. Russo MT, De Luca G, Degan P, Parlanti E, Dogliotti E, Barnes DE, Lindahl T, Yang H, Miller JH, Bignami M. Accumulation of the oxidative base lesion 8-hydroxyguanine in DNA of tumor-prone mice defective in both the myh and ogg1 DNA glycosylases. *Cancer Res*. 2004; 64:4411–4414. [PubMed: 15231648]
16. Torres-Gonzalez M, Gawlowski T, Kocalis H, Scott BT, Dillmann WH. Mitochondrial 8-oxoguanine glycosylase decreases mitochondrial fragmentation and improves mitochondrial

- function in h9c2 cells under oxidative stress conditions. *Am J Physiol Cell Physiol*. 2014; 306:C221–229. [PubMed: 24304833]
17. Ruchko M, Sukhanov S, Gorodnya O, Pastukh V, Danchuk S, Rachek L, Gillespie M. Involvement of mitochondrial (mt) DNA oxidative damage and circulating fragments in early stages of atherogenesis. *Faseb Journal*. 2015; 29
 18. Shirwany NA, Zou MH. Ampk in cardiovascular health and disease. *Acta Pharmacol Sin*. 2010; 31:1075–1084. [PubMed: 20711221]
 19. Dong Y, Zhang M, Liang B, Xie Z, Zhao Z, Asfa S, Choi HC, Zou MH. Reduction of amp-activated protein kinase alpha2 increases endoplasmic reticulum stress and atherosclerosis in vivo. *Circulation*. 2010; 121:792–803. [PubMed: 20124121]
 20. Li Y, Xu S, Jiang B, Cohen RA, Zang M. Activation of sterol regulatory element binding protein and nlrp3 inflammasome in atherosclerotic lesion development in diabetic pigs. *PLoS one*. 2013; 8:e67532. [PubMed: 23825667]
 21. Habib SL, Kasinath BS, Arya RR, Vexler S, Velagapudi C. Novel mechanism of reducing tumorigenesis: Upregulation of the DNA repair enzyme ogg1 by rapamycin-mediated ampk activation and mtor inhibition. *Eur J Cancer*. 2010; 46:2806–2820. [PubMed: 20656472]
 22. Rayner KJ, Sheedy FJ, Esau CC, Hussain FN, Temel RE, Parathath S, van Gils JM, Rayner AJ, Chang AN, Suarez Y, Fernandez-Hernando C, Fisher EA, Moore KJ. Antagonism of mir-33 in mice promotes reverse cholesterol transport and regression of atherosclerosis. *The Journal of clinical investigation*. 2011; 121:2921–2931. [PubMed: 21646721]
 23. Horie T, Baba O, Kuwabara Y, Chujo Y, Watanabe S, Kinoshita M, Horiguchi M, Nakamura T, Chonabayashi K, Hishizawa M, Hasegawa K, Kume N, Yokode M, Kita T, Kimura T, Ono K. MicroRNA-33 deficiency reduces the progression of atherosclerotic plaque in apoE^{-/-} mice. *J Am Heart Assoc*. 2012; 1:e003376. [PubMed: 23316322]
 24. Chen S, Shimada K, Zhang W, Huang G, Crother TR, Arditi M. Il-17a is proatherogenic in high-fat diet-induced and chlamydia pneumoniae infection-accelerated atherosclerosis in mice. *Journal of immunology (Baltimore, Md: 1950)*. 2010; 185:5619–5627.
 25. Trogan E, Choudhury RP, Dansky HM, Rong JX, Breslow JL, Fisher EA. Laser capture microdissection analysis of gene expression in macrophages from atherosclerotic lesions of apolipoprotein e-deficient mice. *Proceedings of the National Academy of Sciences of the United States of America*. 2002; 99:2234–2239. [PubMed: 11842210]
 26. Corral-Debrinski M, Shoffner JM, Lott MT, Wallace DC. Association of mitochondrial DNA damage with aging and coronary atherosclerotic heart disease. *Mutat Res*. 1992; 275:169–180. [PubMed: 1383759]
 27. Ricci C, Pastukh V, Leonard J, Turens J, Wilson G, Schaffer D, Schaffer SW. Mitochondrial DNA damage triggers mitochondrial-superoxide generation and apoptosis. *Am J Physiol Cell Physiol*. 2008; 294:C413–422. [PubMed: 18077603]
 28. Terasaka N, Wang N, Yvan-Charvet L, Tall AR. High-density lipoprotein protects macrophages from oxidized low-density lipoprotein-induced apoptosis by promoting efflux of 7-ketocholesterol via abcg1. *Proceedings of the National Academy of Sciences of the United States of America*. 2007; 104:15093–15098. [PubMed: 17846428]
 29. Lizard G, Lemaire S, Monier S, Gueldry S, Neel D, Gambert P. Induction of apoptosis and of interleukin-1beta secretion by 7beta-hydroxycholesterol and 7-ketocholesterol: Partial inhibition by bcl-2 overexpression. *FEBS Lett*. 1997; 419:276–280. [PubMed: 9428650]
 30. Indaram M, Ma W, Zhao L, Fariss RN, Rodriguez IR, Wong WT. 7-ketocholesterol increases retinal microglial migration, activation, and angiogenicity: A potential pathogenic mechanism underlying age-related macular degeneration. *Sci Rep*. 2015; 5:9144. [PubMed: 25775051]
 31. Ballinger SW, Patterson C, Knight-Lozano CA, Burow DL, Conklin CA, Hu Z, Reuf J, Horaist C, Lebovitz R, Hunter GC, McIntyre K, Runge MS. Mitochondrial integrity and function in atherogenesis. *Circulation*. 2002; 106:544–549. [PubMed: 12147534]
 32. Martinet W, Knaapen MW, De Meyer GR, Herman AG, Kockx MM. Elevated levels of oxidative DNA damage and DNA repair enzymes in human atherosclerotic plaques. *Circulation*. 2002; 106:927–932. [PubMed: 12186795]

33. Wang Y, Wang GZ, Rabinovitch PS, Tabas I. Macrophage mitochondrial oxidative stress promotes atherosclerosis and nuclear factor-kappaB-mediated inflammation in macrophages. *Circulation research*. 2014; 114:421–433. [PubMed: 24297735]
34. Rosenfeld ME. Converting smooth muscle cells to macrophage-like cells with klf4 in atherosclerotic plaques. *Nat Med*. 2015; 21:549–551. [PubMed: 26046571]
35. Liao, X.; Sluimer, JC.; Wang, Y.; Subramanian, M.; Brown, K.; Pattison, JS.; Robbins, J.; Martinez, J.; Tabas, I. *Cell metab*. United States: 2012 Elsevier Inc; 2012. Macrophage autophagy plays a protective role in advanced atherosclerosis; p. 545-553.
36. Wang Y, Tabas I. Emerging roles of mitochondria ros in atherosclerotic lesions: Causation or association? *J Atheroscler Thromb*. 2014; 21:381–390. [PubMed: 24717761]
37. Tedgui A, Mallat Z. Cytokines in atherosclerosis: Pathogenic and regulatory pathways. *Physiol Rev*. 2006; 86:515–581. [PubMed: 16601268]
38. Kleemann R, Zadelaar S, Kooistra T. Cytokines and atherosclerosis: A comprehensive review of studies in mice. *Cardiovasc Res*. 2008; 79:360–376. [PubMed: 18487233]
39. Sampath H, Vartanian V, Rollins MR, Sakumi K, Nakabeppu Y, Lloyd RS. 8-oxoguanine DNA glycosylase (ogg1) deficiency increases susceptibility to obesity and metabolic dysfunction. *PLoS one*. 2012; 7:e51697. [PubMed: 23284747]
40. Fernandez-Hernando C, Suarez Y, Rayner KJ, Moore KJ. Micrnas in lipid metabolism. *Curr Opin Lipidol*. 2011; 22:86–92. [PubMed: 21178770]
41. Moore KJ, Rayner KJ, Suarez Y, Fernandez-Hernando C. Micrnas and cholesterol metabolism. *Trends Endocrinol Metab*. 2010; 21:699–706. [PubMed: 20880716]
42. Rayner KJ, Esau CC, Hussain FN, McDaniel AL, Marshall SM, van Gils JM, Ray TD, Sheedy FJ, Goedeke L, Liu X, Khatsenko OG, Kaimal V, Lees CJ, Fernandez-Hernando C, Fisher EA, Temel RE, Moore KJ. Inhibition of mir-33a/b in non-human primates raises plasma hdl and lowers vldl triglycerides. *Nature*. 2011; 478:404–407. [PubMed: 22012398]
43. Karunakaran D, Thrush AB, Nguyen MA, Richards L, Geoffrion M, Singaravelu R, Ramphos E, Shangari P, Ouimet M, Pezacki JP, Moore KJ, Perisic L, Maegdefessel L, Hedin U, Harper ME, Rayner KJ. Macrophage mitochondrial energy status regulates cholesterol efflux and is enhanced by anti-mir33 in atherosclerosis. *Circulation research*. 2015; 117:266–278. [PubMed: 26002865]
44. Shyu HY, Shieh JC, Ji-Ho L, Wang HW, Cheng CW. Polymorphisms of DNA repair pathway genes and cigarette smoking in relation to susceptibility to large artery atherosclerotic stroke among ethnic chinese in taiwan. *J Atheroscler Thromb*. 2012; 19:316–325. [PubMed: 22277767]
45. Lee HT, Lin CS, Lee CS, Tsai CY, Wei YH. The role of hogg1 c1245g polymorphism in the susceptibility to lupus nephritis and modulation of the plasma 8-ohdg in patients with systemic lupus erythematosus. *International journal of molecular sciences*. 2015; 16:3757–3768. [PubMed: 25671815]
46. Lee HT, Lin CS, Lee CS, Tsai CY, Wei YH. Increased 8-hydroxy-2'-deoxyguanosine in plasma and decreased mrna expression of human 8-oxoguanine DNA glycosylase 1, anti-oxidant enzymes, mitochondrial biogenesis-related proteins and glycolytic enzymes in leucocytes in patients with systemic lupus erythematosus. *Clin Exp Immunol*. 2014; 176:66–77. [PubMed: 24345202]
47. Kockx MM, Herman AG. Apoptosis in atherosclerosis: Beneficial or detrimental? *Cardiovasc Res*. 2000; 45:736–746. [PubMed: 10728396]
48. Bacsı A, Chodaczek G, Hazra TK, Konkel D, Boldogh I. Increased ros generation in subsets of ogg1 knockout fibroblast cells. *Mechanisms of ageing and development*. 2007; 128:637–649. [PubMed: 18006041]
49. Ruchko MV, Gorodnya OM, Zuleta A, Pastukh VM, Gillespie MN. The DNA glycosylase ogg1 defends against oxidant-induced mtdna damage and apoptosis in pulmonary artery endothelial cells. *Free radical biology & medicine*. 2011; 50:1107–1113. [PubMed: 20969951]
50. Ruchko M, Gorodnya O, LeDoux SP, Alexeyev MF, Al-Mehdi AB, Gillespie MN. Mitochondrial DNA damage triggers mitochondrial dysfunction and apoptosis in oxidant-challenged lung endothelial cells. *Am J Physiol Lung Cell Mol Physiol*. 2005; 288:L530–535. [PubMed: 15563690]
51. Cha MY, Kim DK, Mook-Jung I. The role of mitochondrial DNA mutation on neurodegenerative diseases. *Exp Mol Med*. 2015; 47:e150. [PubMed: 25766619]

52. Tuppen HA, Blakely EL, Turnbull DM, Taylor RW. Mitochondrial DNA mutations and human disease. *Biochim Biophys Acta*. 2010; 1797:113–128. [PubMed: 19761752]
53. Liao X, Sluimer JC, Wang Y, Subramanian M, Brown K, Pattison JS, Robbins J, Martinez J, Tabas I. Macrophage autophagy plays a protective role in advanced atherosclerosis. *Cell Metab*. 2012; 15:545–553. [PubMed: 22445600]
54. Tabas I. Macrophage death and defective inflammation resolution in atherosclerosis. *Nature reviews Immunology*. 2010; 10:36–46.
55. Tabas I. Consequences and therapeutic implications of macrophage apoptosis in atherosclerosis: The importance of lesion stage and phagocytic efficiency. *Arteriosclerosis, Thrombosis, and Vascular Biology*. 2005; 25:2255–2264.
56. Croteau DL, Bohr VA. Repair of oxidative damage to nuclear and mitochondrial DNA in mammalian cells. *Journal of Biological Chemistry*. 1997; 272:25409–25412. [PubMed: 9325246]
57. Bohr VA. Repair of oxidative DNA damage in nuclear and mitochondrial DNA, and some changes with aging in mammalian cells. *Free radical biology & medicine*. 2002; 32:804–812. [PubMed: 11978482]
58. Madamanchi NR, Runge MS. Mitochondrial dysfunction in atherosclerosis. *Circulation research*. 2007; 100:460–473. [PubMed: 17332437]
59. de Souza-Pinto NC, Eide L, Hogue BA, Thybo T, Stevnsner T, Seeberg E, Klungland A, Bohr VA. Repair of 8-oxodeoxyguanosine lesions in mitochondrial dna depends on the oxoguanine dna glycosylase (ogg1) gene and 8-oxoguanine accumulates in the mitochondrial dna of ogg1-defective mice. *Cancer research*. 2001; 61:5378–5381. [PubMed: 11454679]
60. Janik J, Swoboda M, Janowska B, Ciesla JM, Gackowski D, Kowalewski J, Olinski R, Tudek B, Speina E. 8-oxoguanine incision activity is impaired in lung tissues of nscl patients with the polymorphism of ogg1 and xrcc1 genes. *Mutat Res*. 2011:709–710. 21–31.
61. Stuart JA, Bourque BM, de Souza-Pinto NC, Bohr VA. No evidence of mitochondrial respiratory dysfunction in ogg1-null mice deficient in removal of 8-oxodeoxyguanine from mitochondrial DNA. *Free Radic Biol Med*. 2005; 38:737–745. [PubMed: 15721984]
62. Vandanmagsar B, Youm YH, Ravussin A, Galgani JE, Stadler K, Mynatt RL, Ravussin E, Stephens JM, Dixit VD. The nlrp3 inflammasome instigates obesity-induced inflammation and insulin resistance. *Nat Med*. 2011; 17:179–188. [PubMed: 21217695]
63. Wen H, Gris D, Lei Y, Jha S, Zhang L, Huang MT, Brickey WJ, Ting JP. Fatty acid-induced nlrp3-asc inflammasome activation interferes with insulin signaling. *Nature immunology*. 2011; 12:408–415. [PubMed: 21478880]
64. Kirii H, Niwa T, Yamada Y, Wada H, Saito K, Iwakura Y, Asano M, Moriwaki H, Seishima M. Lack of interleukin-1beta decreases the severity of atherosclerosis in apoe-deficient mice. *Arteriosclerosis, thrombosis, and vascular biology*. 2003; 23:656–660.
65. Ozaki E, Campbell M, Doyle SL. Targeting the nlrp3 inflammasome in chronic inflammatory diseases: Current perspectives. *J Inflamm Res*. 2015; 8:15–27. [PubMed: 25653548]
66. Lu X, Kakkar V. Inflammasome and atherogenesis. *Curr Pharm Des*. 2014; 20:108–124. [PubMed: 23944376]
67. Boldogh I, Hajas G, Aguilera-Aguirre L, Hegde ML, Radak Z, Bacsi A, Sur S, Hazra TK, Mitra S. Activation of ras signaling pathway by 8-oxoguanine DNA glycosylase bound to its excision product, 8-oxoguanine. *J Biol Chem*. 2012; 287:20769–20773. [PubMed: 22568941]
68. Hashizume M, Mouner M, Chouteau JM, Gorodnya OM, Ruchko MV, Potter BJ, Wilson GL, Gillespie MN, Parker JC. Mitochondrial-targeted DNA repair enzyme 8-oxoguanine DNA glycosylase 1 protects against ventilator-induced lung injury in intact mice. *Am J Physiol Lung Cell Mol Physiol*. 2013; 304:L287–297. [PubMed: 23241530]
69. Ramirez CM, Goedeke L, Rotllan N, Yoon JH, Cirera-Salinas D, Mattison JA, Suarez Y, de Cabo R, Gorospe M, Fernandez-Hernando C. MicroRNA 33 regulates glucose metabolism. *Mol Cell Biol*. 2013; 33:2891–2902. [PubMed: 23716591]
70. Rayner KJ, Fernandez-Hernando C, Moore KJ. MicroRNAs regulating lipid metabolism in atherogenesis. *Thromb Haemost*. 2012; 107:642–647. [PubMed: 22274626]
71. Madrigal-Matute J, Rotllan N, Aranda JF, Fernandez-Hernando C. MicroRNAs and atherosclerosis. *Curr Atheroscler Rep*. 2013; 15:322. [PubMed: 23512606]

72. Moore KJ, Rayner KJ, Suarez Y, Fernandez-Hernando C. MicroRNAs and cholesterol metabolism. *Trends Endocrinol Metab.* 2010; 21:699–706. [PubMed: 20880716]
73. Karunakaran D, Thrush AB, Nguyen M-A, Richards L, Geoffrion M, Singaravelu R, Ramphos E, Shangari P, Ouimet M, Pezacki JP, Moore KJ, Perisic L, Maegdefessel L, Hedin U, Harper M-E, Rayner KJ. Macrophage mitochondrial energy status regulates cholesterol efflux and is enhanced by anti-mir33 in atherosclerosis. *Circulation Research.* 2015; 117:266–278. [PubMed: 26002865]
74. Price NL, Fernandez-Hernando C. Novel role of mir-33 in regulating of mitochondrial function. *Circulation research.* 2015; 117:225–228. [PubMed: 26185207]
75. Ouimet M, Ediriweera HN, Gundra UM, Sheedy FJ, Ramkhelawon B, Hutchison SB, Rinehold K, van Solingen C, Fullerton MD, Cecchini K, Rayner KJ, Steinberg GR, Zamore PD, Fisher EA, Loke P, Moore KJ. MicroRNA-33-dependent regulation of macrophage metabolism directs immune cell polarization in atherosclerosis. *The Journal of clinical investigation.* 2015; 125:4334–4348. [PubMed: 26517695]
76. Distel E, Barrett TJ, Chung K, Girgis NM, Parathath S, Essau CC, Murphy AJ, Moore KJ, Fisher EA. Mir33 inhibition overcomes deleterious effects of diabetes mellitus on atherosclerosis plaque regression in mice. *Circulation research.* 2014; 115:759–769. [PubMed: 25201910]
77. Goedeke L, Salerno A, Ramirez CM, Guo L, Allen RM, Yin X, Langley SR, Esau C, Wanschel A, Fisher EA, Suarez Y, Baldan A, Mayr M, Fernandez-Hernando C. Long-term therapeutic silencing of mir-33 increases circulating triglyceride levels and hepatic lipid accumulation in mice. *EMBO Mol Med.* 2014; 6:1133–1141. [PubMed: 25038053]
78. Rotllan N, Ramirez CM, Aryal B, Esau CC, Fernandez-Hernando C. Therapeutic silencing of microRNA-33 inhibits the progression of atherosclerosis in *ldlr*^{-/-} mice—brief report. *Arteriosclerosis, thrombosis, and vascular biology.* 2013; 33:1973–1977.
79. Cheng J, Qiao L, Xu X, Zhai C, Zhao K, Ji X, Chen W. Lower amp-activated protein kinase level is associated with the vulnerability of coronary atherosclerotic plaques by attenuating the expression of monocyte autophagy. *Coron Artery Dis.* 2015; 26:322–327. [PubMed: 25768243]
80. Li Y, Xu S, Mihaylova MM, Zheng B, Hou X, Jiang B, Park O, Luo Z, Lefai E, Shyy JY, Gao B, Wierzbicki M, Verbeuren TJ, Shaw RJ, Cohen RA, Zang M. Ampk phosphorylates and inhibits srebp activity to attenuate hepatic steatosis and atherosclerosis in diet-induced insulin-resistant mice. *Cell Metab.* 2011; 13:376–388. [PubMed: 21459323]
81. Zang M, Xu S, Maitland-Toolan KA, Zuccollo A, Hou X, Jiang B, Wierzbicki M, Verbeuren TJ, Cohen RA. Polyphenols stimulate amp-activated protein kinase, lower lipids, and inhibit accelerated atherosclerosis in diabetic *ldl* receptor-deficient mice. *Diabetes.* 2006; 55:2180–2191. [PubMed: 16873680]
82. Forouzandeh F, Salazar G, Patrushev N, Xiong S, Hilenski L, Fei B, Alexander RW. Metformin beyond diabetes: Pleiotropic benefits of metformin in attenuation of atherosclerosis. *J Am Heart Assoc.* 2014; 3:e001202. [PubMed: 25527624]
83. Lee MR, Kim SH, Cho HJ, Lee KY, Moon AR, Jeong HG, Lee JS, Hyun JW, Chung MH, You HJ. Transcription factors *nf-ya* regulate the induction of human *ogg1* following DNA-alkylating agent methylmethane sulfonate (mms) treatment. *J Biol Chem.* 2004; 279:9857–9866. [PubMed: 14688259]
84. Bartz RR, Suliman HB, Fu P, Welty-Wolf K, Carraway MS, MacGarvey NC, Withers CM, Sweeney TE, Piantadosi CA. Staphylococcus aureus sepsis and mitochondrial accrual of the 8-oxoguanine DNA glycosylase DNA repair enzyme in mice. *American journal of respiratory and critical care medicine.* 2011; 183:226–233. [PubMed: 20732986]
85. Salminen A, Kaamiranta K. Amp-activated protein kinase (ampk) controls the aging process via an integrated signaling network. *Ageing research reviews.* 2012; 11:230–241. [PubMed: 22186033]
86. Randolph GJ. Mechanisms that regulate macrophage burden in atherosclerosis. *Circulation research.* 2014; 114:1757–1771. [PubMed: 24855200]
87. Yakes FM, VanHouten B. Mitochondrial DNA damage is more extensive and persists longer than nuclear DNA damage in human cells following oxidative stress. *Proceedings of the National Academy of Sciences of the United States of America.* 1997; 94:514–519. [PubMed: 9012815]

88. Botto N, Rizza A, Colombo MG, Mazzone AM, Manfredi S, Masetti S, Clerico A, Biagini A, Andreassi MG. Evidence for DNA damage in patients with coronary artery disease. *Mutation Research/Genetic Toxicology and Environmental Mutagenesis*. 2001; 493:23–30.

Author Manuscript

Author Manuscript

Author Manuscript

Author Manuscript

Novelty and Significance

What Is Known?

- Mitochondrial DNA damage has been implicated in NLRP3 inflammasome activation and in atherogenesis, and is increased in human atherosclerotic plaques.
- OGG1 (oxy-guanine glycosylase 1) is the main enzyme responsible for repairing mitochondrial oxidative DNA damage.
- miR-33 negatively regulates several anti-atherosclerotic pathways and is considered to be a potential anti-atherosclerosis therapeutic target.

What New Information Does This Article Contribute?

- Loss of OGG1 leads to increased mitochondrial DNA damage and NLRP3 inflammasome activation in plaque macrophages.
- This study shows that OGG1 plays a protective role in atherogenesis by preventing excessive inflammasome activation.
- OGG1 is reduced in plaque macrophages as the lesion progresses and is negatively regulated by the proatherogenic miR-33.

Recent evidence suggests that oxidative stress and mitochondrial DNA (mtDNA) damage is present in atherosclerotic plaques, directly promoting NLRP3 inflammasome activation and multiple pro-atherogenic processes through mitochondrial dysfunction. Using mice deficient in both OGG1 and the LDL receptor (LDLR) we found that; 1) genetic deletion of OGG1 leads to larger and more advanced plaques; 2) increased accumulation of the oxidative DNA damage product 8-OH-dG localized to the mitochondria of plaque macrophages; and 3) increased caspase-1 activation. By using OGG1/NLRP3 double knockout mice as donors for bone marrow chimera experiments we found that the OGG1 deficiency-mediated increase in atherosclerotic plaque progression was predominately NLRP3-dependent. We observed that OGG1 expression diminishes in atherosclerotic plaque macrophages in mice as the lesion progresses and in human atherosclerotic plaques. Finally, we discovered that miR-33, a proathogenic microRNA, which is known to be increased in atherosclerotic lesions, downregulates OGG1 expression. These findings demonstrate that OGG1 is atheroprotective and that targeting mtDNA repair may provide a new strategy for reducing plaque development by harnessing pre-existing protective processes.

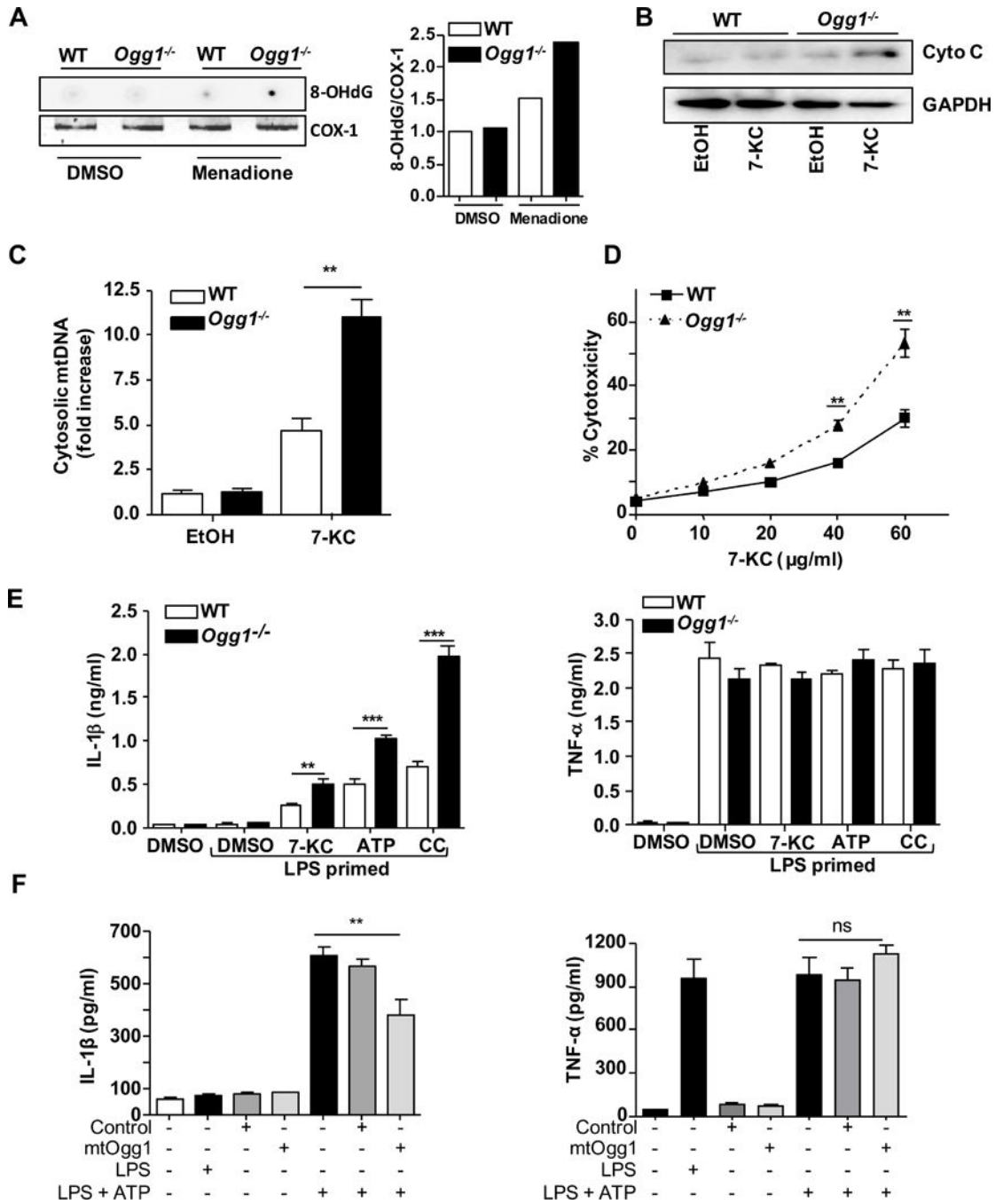


Figure 1. OGG1-deficient macrophages are more apoptotic and inflammatory
(A) The level of 8-OHdG in mtDNA. BMDM derived from WT or *Ogg1*^{-/-} mice were stimulated with ROS inducer (menadione 25 μM for 30 min), followed by 2h incubation to allow for DNA repair. mtDNA was extracted and 8-OH-dG was measured by dot blot analysis and COX-1 PCR served as a loading control. Densitometry is shown in the right panel. Similar results were observed in 3 independent experiments. **(B–C)** BMDM derived from WT or *Ogg1*^{-/-} mice were stimulated with 40 μg/ml 7-KC or control for (4 h). **(B)** Cytochrome *c* release into the cytosol was assessed by Western blot analysis. Similar results

were observed in 3 independent experiments. **(C)** mtDNA content in the cytosol was assessed by RT-PCR. **(D)** Cell viability was determined by MTT assay after indicated doses of 7-KC treatment for 24 h. **(E)** 4 h LPS-primed BMDM from WT or *Ogg1*^{-/-} mice were stimulated with 5 mM ATP (1 h), 20 µg/ml 7-KC (6 h), or 2 mg/ml cholesterol crystals (16 h). IL-1β and TNF-α concentrations in the culture supernatant were determined by ELISA. **(F)** *Ogg1* KO BMDM cells were transduced with control and mtOgg1 expressing retrovirus for 48 h before the treatment of 400 ng/ml of LPS for 4 h plus 5 mM of ATP in the last hour. IL-1β and TNF-α concentrations in the culture supernatant were determined by ELISA. (C–F) All data are mean±SD and representative of 3 independent experiments in triplicate. Significance was determined using Student's *t*-test **p*<0.05, ***p*<0.01, ****p*<0.001.

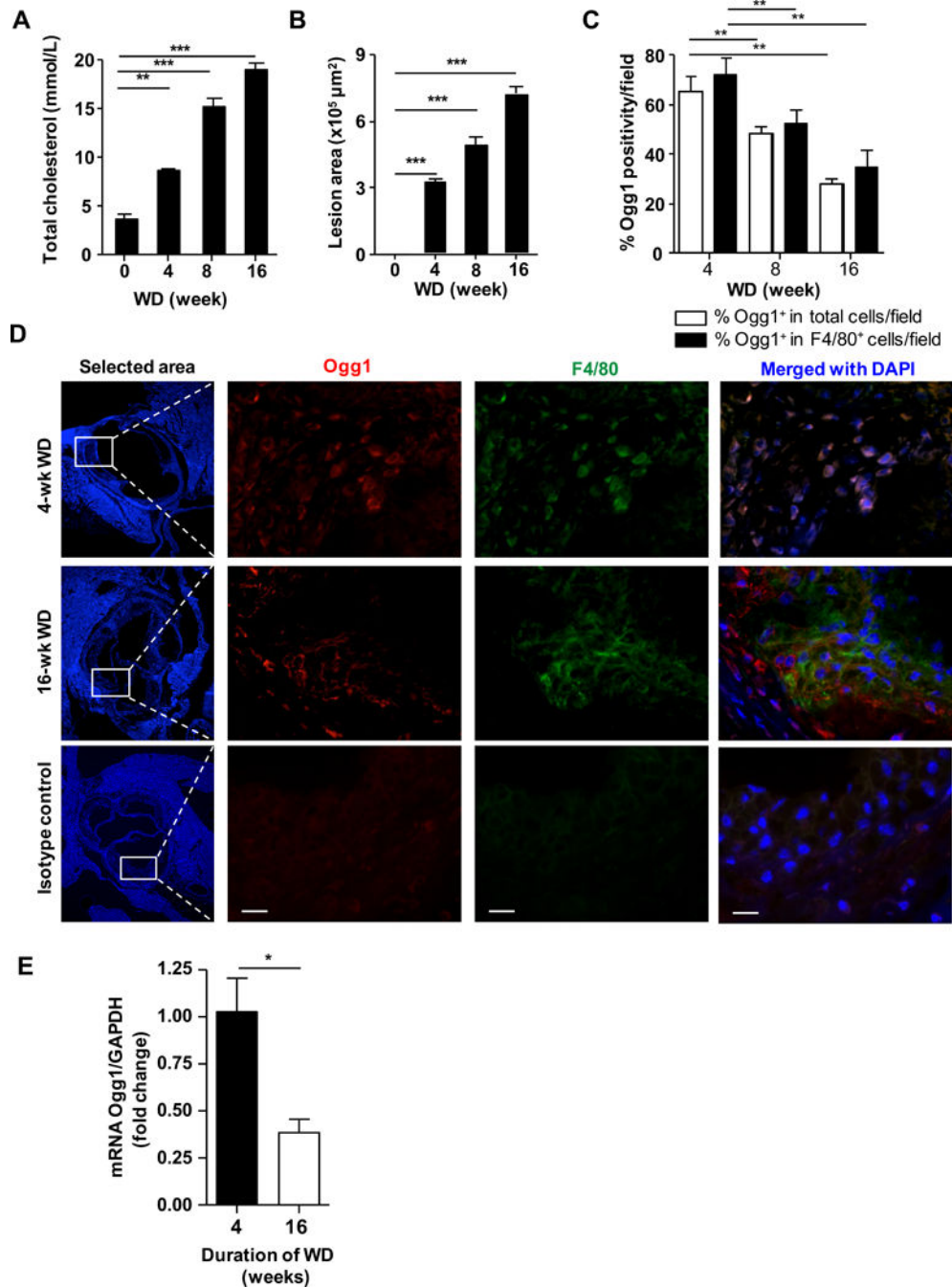


Figure 2. The expression of OGG1 diminishes in macrophages in atherosclerotic lesions overtime *Ldlr*^{-/-} mice fed western diet for 0, 4, 8 or 16 weeks (n=6 per group). **(A)** Total plasma cholesterol concentrations. All data are mean \pm SD and each sample in duplicate. **(B)** Quantification of aortic root plaque area. **(C)** Quantification of OGG1⁺ cells within aortic root plaque as measured by immunofluorescence. **(D)** Representative images of immunofluorescent staining for OGG1 in aortic root plaques. Macrophage marker F4/80 (green), Nuclei (blue) and OGG1 (red). Magnification 40 \times . Scale bar = 20 μm . **(E)** Expression of *Ogg1* mRNA in plaque F4/80⁺ macrophages isolated by laser-capture

microdissection and analyzed by qRT-PCR. All data are mean±SD and representative of 2 independent experiments in triplicate. Significance was determined using One-Way ANOVA with Tukey's post-hoc test. * $p<0.05$, ** $p<0.01$, *** $p<0.001$.

Author Manuscript

Author Manuscript

Author Manuscript

Author Manuscript

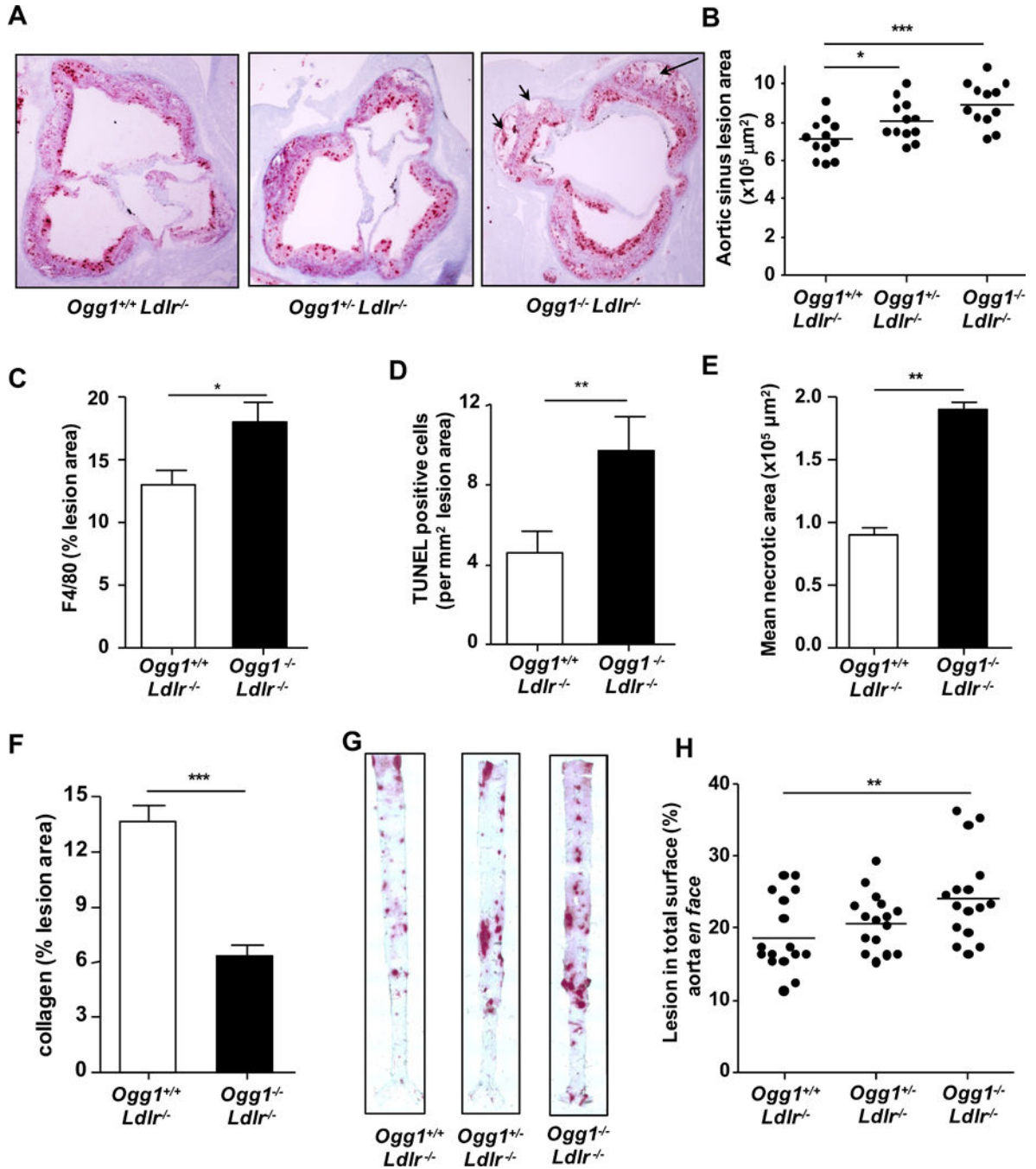


Figure 3. OGG1 deficiency leads to accelerated atherosclerosis in LDLR-deficient mice
Ogg1^{-/-}*Ldlr*^{-/-}, *Ogg1*^{+/-}*Ldlr*^{-/-} and control *Ogg1*^{+/+}*Ldlr*^{-/-} mice were fed WD for 16 weeks (n=12). (A) Representative pictures of aortic root plaques stained with Oil Red O (40×). *Black arrows* show necrotic cellular areas. (B) Aortic root plaques area quantification. (C) Macrophage content. (D) Quantification of TUNEL positivity area (E) Necrotic core area in aortic root lesions (F) Percent collagen staining of aortic root using Mason's Trichrome stain. (G) Representative images of aorta *en face* stained with Oil Red O. (H) Quantification of aortic *en face* lesion area (n=16). All data are mean±SD. Significance was

determined using Student's *t*-test and One-Way ANOVA with Tukey's post-hoc test.
p*<0.05, *p*<0.01, ****p*<0.001.

Author Manuscript

Author Manuscript

Author Manuscript

Author Manuscript

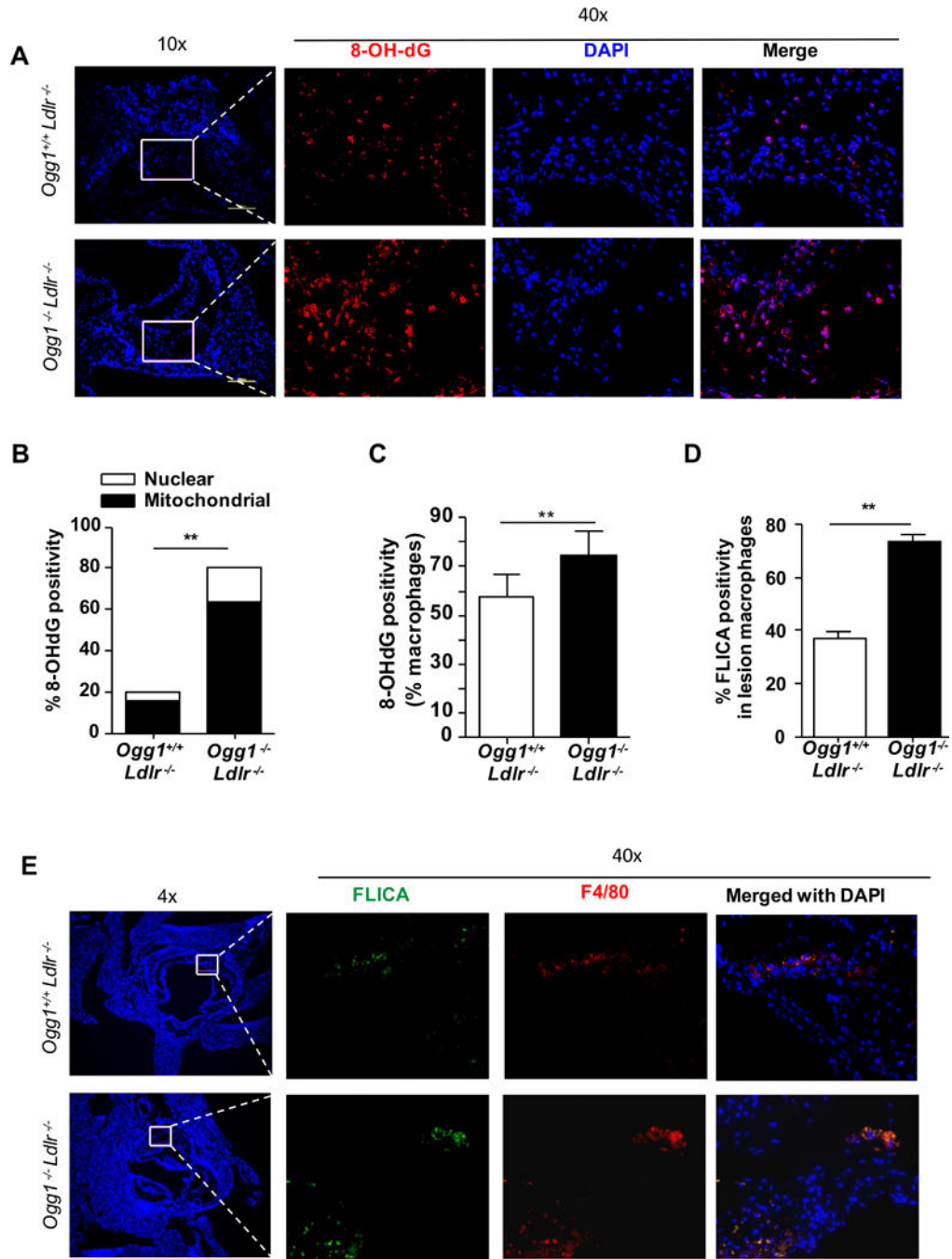


Figure 4. OGG1 deficiency leads to increased oxidative DNA damage (8-OH-dG) dominantly in mitochondria and caspase-1 activity in macrophages atherosclerotic lesions

Ogg1^{-/-}Ldlr^{-/-} and control *Ogg1^{+/+}Ldlr^{-/-}* mice were fed WD for 16 weeks. Aortic root plaques were analyzed by immunofluorescence. (A) DNA damage was measured by immunostaining for 8-OH-dG (red) and nuclei (blue). (B) Quantitative analysis of 8-OH-dG⁺ cells in selected area. Increased 8-OH-dG found mainly in mitochondria (TOM20) (C) 8-OH-dG positive macrophages in lesion. (D) Quantification of active caspase-1⁺ cells in lesional macrophages. (E) Caspase-1 activity was assessed by FLICA (green) and by

labelling macrophages with anti-F4/80 (red) and nuclei (blue). All data (in B, C, and D) are mean \pm SD and representative of 2 independent experiments (n=10). Significance was determined using Student's *t*-test. ** $p<0.01$.

Author Manuscript

Author Manuscript

Author Manuscript

Author Manuscript

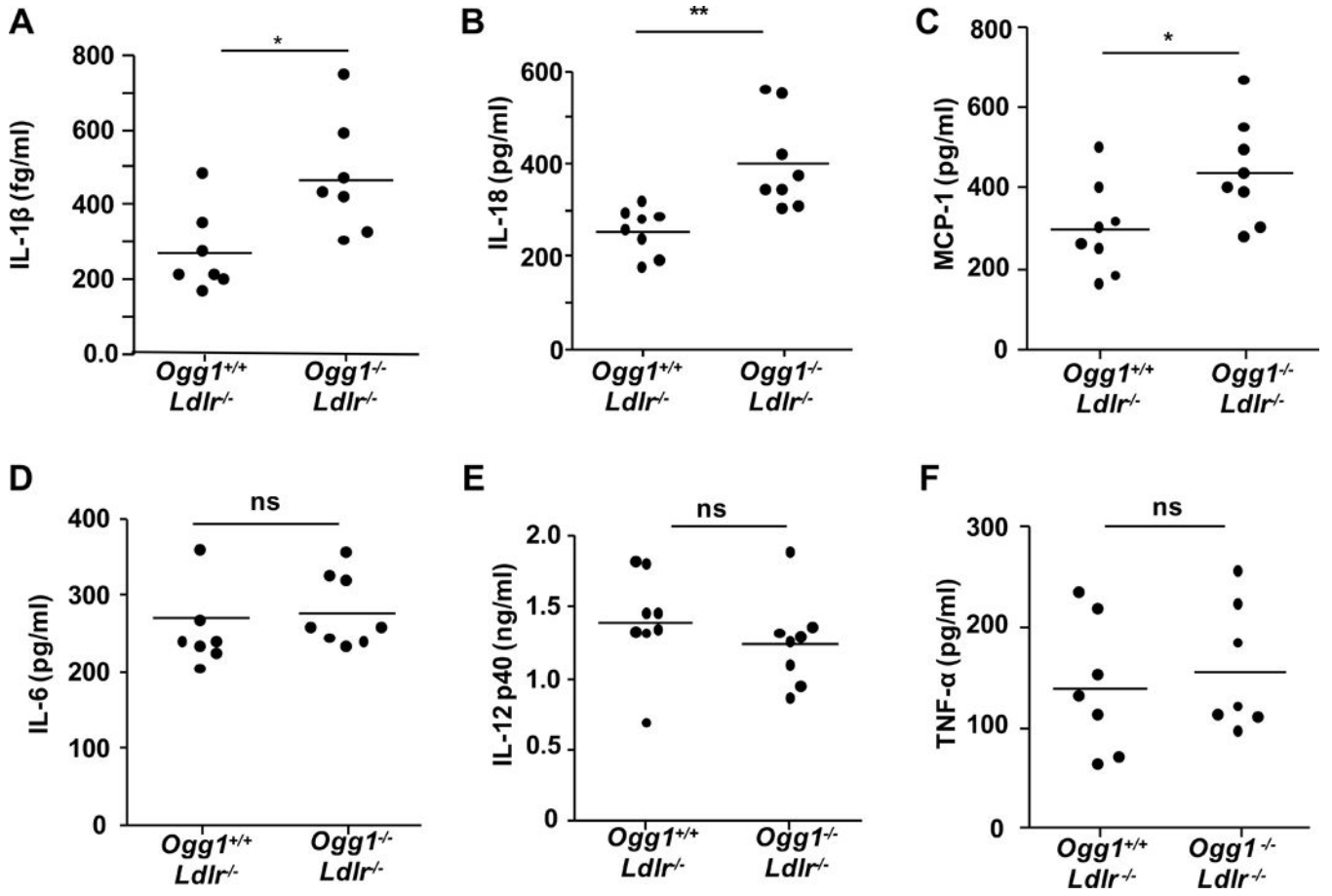


Figure 5. Plasma levels of cytokines and chemokines

(A–D) Plasma concentrations of IL-1 β measured by MSD and IL-18, MCP-1, IL-6, IL-12p40 and TNF- α were detected by ELISA (n=7–8). All data are expressed as mean \pm SD and performed in triplicate. Student's *t*-test was used **p*<0.05. ns= not significant.

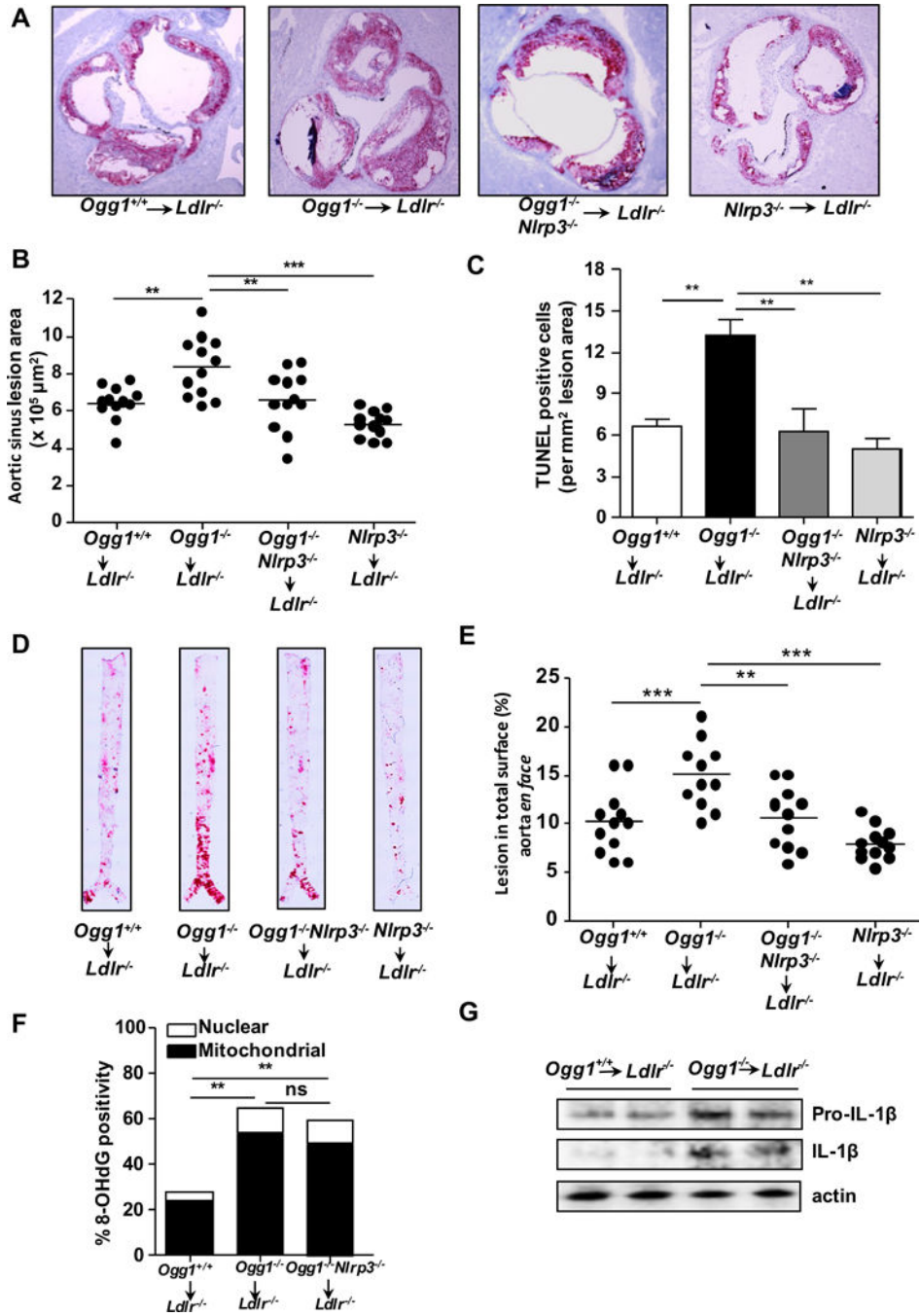


Figure 6. NLRP3 is required for OGG1 deficiency-induced acceleration of atherosclerosis in hematopoietic cells

BM from WT, *Ogg1^{-/-}*, *Ogg1^{-/-}Nlrp3^{-/-}*, or *Nlrp3^{-/-}* mice were transferred into irradiated *Ldlr^{-/-}* mice and after 8 week reconstitution, mice were fed a WD for 12 weeks (n=11–12). (A) Representative Oil Red O staining of aortic root plaques (10×). (B) Quantification of aortic root lesion area. (C) Quantification of TUNEL positivity (D) Representative images of Oil Red O staining on Aorta *en face*. (E) Quantification of aortic *en face* lesion area. (F) Quantification of 8-OH-dG positivity in aortic root plaque by immunofluorescent staining.

(G) Mature IL-1 β in the aortic arch. Each lane represents the pooled aortic arch from 2 mice lysates and analyzed by western blot for IL-1 β . All data are mean \pm SD. Significance was determined using One-Way ANOVA with Tukey's post-hoc test (**B, C, E, and F**). * p <0.05, ** p <0.01.

Author Manuscript

Author Manuscript

Author Manuscript

Author Manuscript

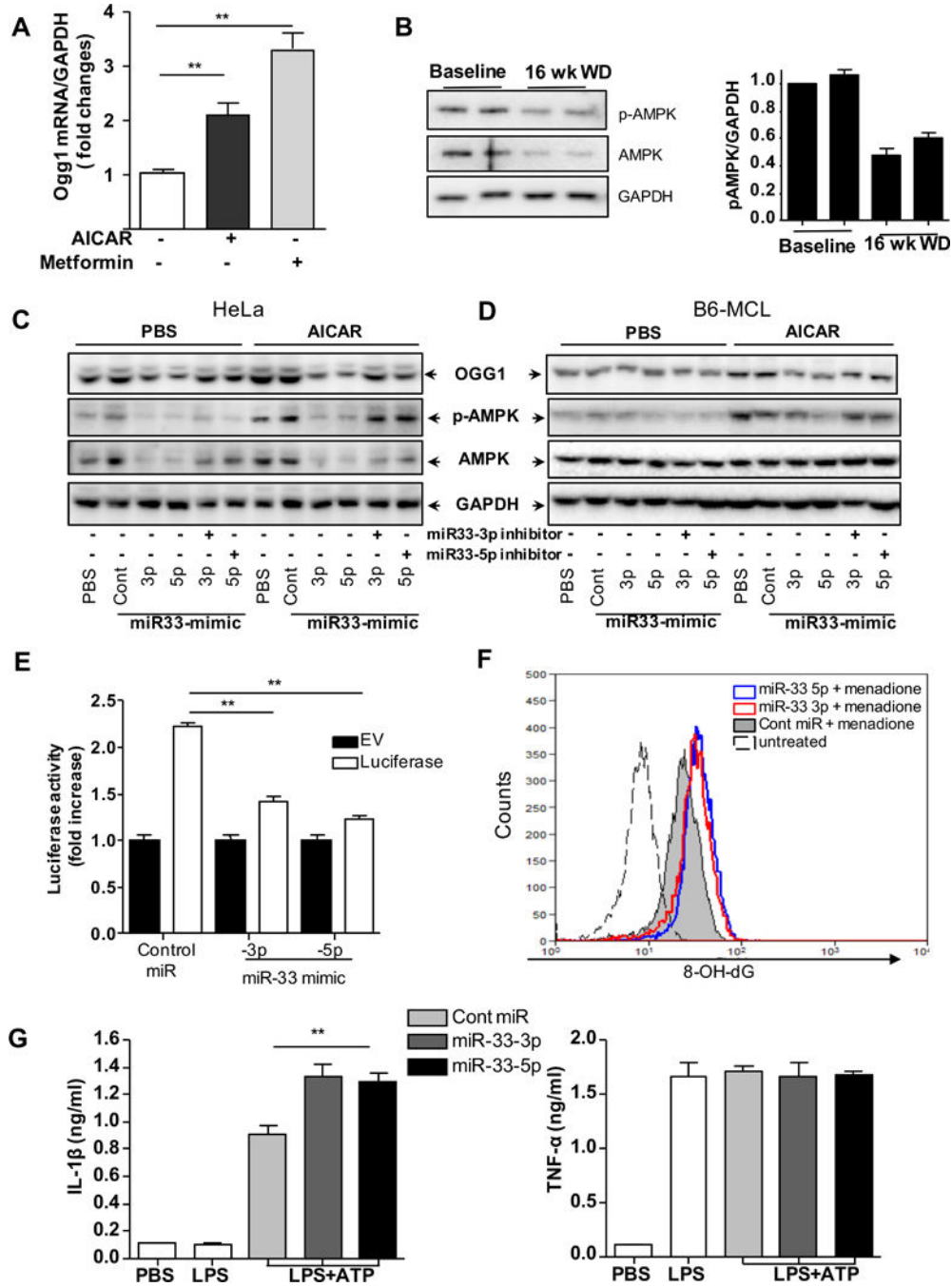


Figure 7. The regulation of *Ogg1* expression

(A) mRNA *Ogg1* expression was examined by RT-PCR. The cells were treated with AMPK activators (1 mM AICAR for 4 h and 7.5 μM Metformin for 8h). (B) p-AMPK and AMPK protein in the aortic arch. Each lane represents the pooled aortic arch lysates from two *Ldlr*^{-/-} mice and analyzed by western blot. GAPDH used as a loading control. Band densitometry is shown in the right panel. (C and D) Western blot analysis of *Ogg1*, p-AMPK, AMPK and GAPDH protein expression transfected with the control mimic (control), miR-33-3p and -5p mimics, and/or mimic inhibitors for 48 h treated with or

without 1 mM AICAR for 2 h. **(E)** Luciferase reporter activity in HEK 293 co transfected with the miR control, miR-33a -3p and -5p with Luciferase reporter (contains 3' UTR of *OGG1* (human)) plasmid for 48 h. **(F)** HEK 293 cells were transfected with miR-33-3p and -5p mimic and control miRNA before 25 μ M menadione (ROS inducer) treatment for 30 min, followed by 4hr incubation to allow for DNA repair. DNA damage was measured by intracellular immunostaining for 8-OH-dG and measured by flow cytometry. **(B–D and F)** Similar results were observed in 3 independent experiments. **(G)** MCL cells were transfected with control miR, miR-33-3p and miR-33-5p mimic for 48 h before the treatment of 400 ng/ml of LPS for 4 h plus 5 mM of ATP in the last hour. **(A, E, and G)** All data are means \pm SD and representative of 3 experiments in duplicate. Significance was determined using One-Way ANOVA with Tukey's post-hoc test. ** $p < 0.01$.